Relaxation mechanisms in a benzyl chloride–toluene glass

Lei Wu*
The James Franck Institute and The Department of Physics, The University of Chicago, Chicago, Illinois 60637
(Received 29 October 1990)

Using frequency-dependent dielectric susceptibility, we have studied three different types of relaxation phenomena, namely primary (α), secondary (β), and conductivity (c) relaxation, in a sample of 25 vol % benzyl chloride in toluene. The measurement covers ten decades of frequency: $10^{-3} < \nu < 10^{7}$ Hz. The conductivity relaxation which is due to mobile ionic impurities in the sample has characteristics similar to those of the primary relaxation. Using the universal scaling curve for the primary relaxation response in glasses, we can separate the primary and secondary relaxations which overlap in frequency. The shape of the secondary relaxation is log-normal in the frequency domain and corresponds to a Gaussian distribution of energy barriers. The relaxation time for this process can be fitted by an Arrhenius form. Extrapolating the data to higher temperatures, we find that it crosses the primary-relaxation curve. We compare a set of similar molecular liquids and conclude that the secondary relaxation is mainly due to the rotation of a subgroup in the benzyl chloride molecule. We also report a measurement of the nonlinear dielectric response. There is no evidence of a divergent nonlinear susceptibility as the glass transition is approached.

I. INTRODUCTION

Several different kinds of relaxation phenomena have been identified in glassy systems. There are relaxations that occur in the supercooled liquid in the region where the viscosity increases dramatically with decreasing temperature. These are known as the primary or α relaxations. At lower temperatures, in the region where the sample is already solid, there is another relaxation mechanism known as secondary or β relaxation. Finally, if there are any mobile ions in the liquid there will be relaxation due to the conductivity, which we call c relaxation. In this paper we study these three different relaxations in one sample, a mixture of 25 vol % benzyl chloride in toluene, and try to understand the relation between the three different relaxation mechanisms. We have chosen the dielectric response as our probe of the dynamics in the glass because of the ease and precision with which these measurements can be made on a single specimen over a wide range of frequency and temperature. Our techniques allow us to cover ten decades of frequency.

As liquids are cooled down below their freezing point, the relaxation time for structural rearrangement increases dramatically. If crystallization can be avoided by sufficiently rapid cooling, most supercooled liquids will enter a metastable glass state. The glass transition is characterized by a large viscosity, typically on the order of 10^{15} poise.[1] This implies a relaxation time on the order of a day. These primary relaxations have been intensively studied for many years by means of specific heat,[2] dielectric[3,4] and mechanical[5,6] spectroscopies, and by viscosity measurements[7,8] (the average shear relaxation time τ is given by the Maxwell relation $\eta = G_\infty \tau$, where G_∞ is the infinite-frequency shear modulus and η is the viscosity). For most glass-forming liquids, the relaxation time τ can be fitted near the glass transition with the empirical Vogel-Tamman-Fulcher equation, $\tau = \tau_0 \exp[A/(T - T_0)]$.

Relaxation spectra are often much more complicated than would be obtained from a simple Debye process, where the response to a step-function perturbation, $\phi(t)$, is given by $\phi(t) = \phi_0 e^{-t/\tau}$. Experiments on relaxation phenomena therefore focus not only on the mean relaxation time but also on the shape of the spectra. If the experiment is done in the frequency domain, the response is given by the Fourier transform of $-d\phi(t)/dt$. Several functional forms for the decay have been introduced as good approximations to the experimental data. One of the more commonly used functions has been the stretched-exponential form: $\phi(t) = \phi_0 \exp[-(t/\tau)^\beta]$, with $0 < \beta < 1$. There is no simple analytic form for this function in the frequency domain. The frequency dependence of the loss spectrum for stretched-exponential decay is broader than that for a Debye function ($\beta = 1$). This form is generally successful in describing relaxation processes for $t \geq \tau$ (or $\omega \leq 1/\tau$). Recently a careful study[4] of several different glass-forming supercooled liquids over a wide frequency range (14 decades) has shown that the high-frequency tail is different from that given by the stretched-exponential form. The data can be scaled onto a simple universal curve for the α relaxation which is independent of temperature for all the samples studied. Only two parameters, the peak frequency and width, are necessary to determine the spectrum for each sample at each temperature.

Secondary, or β, relaxation, takes place at high frequency[9] usually at temperatures well below the glass transition. However, this relaxation can also exist in the equilibrium liquid above T_g. This secondary relaxation has been studied in many glassy systems. However, we still lack knowledge of the detailed frequency dependence and shape of the response function. From the studies of

glassy crystals such as $(KBr)_{1-x}(KCN)_x$,[10,11] we have learned that β relaxation plays a very important role in the properties of glasses and may be a key to the connection between the low-temperature thermal properties and the high-temperature glass transition. It is difficult to get reliable data for this relaxation process not only because there is a much weaker signal and a much broader spectrum than for the α relaxation, but also because α and β relaxations overlap; it is often difficult to disentangle the contributions from these two processes. Because we have a universal curve for the shape of the α relaxations over the entire frequency range,[4] we are now in a position to separate the two different relaxations. Another important issue, the origin of the β relaxation, is still not clear. One explanation of this phenomenon in molecular glasses has been in terms of local motion, internal to a single molecule, which remains active even when the translational motion of the molecules has been frozen out. Alternatively, Goldstein[12] has suggested that β relaxation is an intrinsic property of the glass state and is due to local rearrangements in some minimum of the potential-energy surface in random close-packed systems. This model predicts that the α- and β-relaxation rate should merge above T_g. We have found that the loss peak of the β relaxation, after separating the contribution of the α-relaxation processes, has a very broad log-normal form and that the temperature dependence of the β-relaxation time is of Arrhenius form. At high temperatures it crosses the curve for the α-relaxation processes.

At high temperatures a third relaxation process due to the conductivity of mobile ions in the liquid becomes important. It has been suggested that the mechanism for ionic conduction and for the mobile cation self-diffusion coefficient (responsible for the viscosity) are identical.[13] This was seen in the motion of small molecules in the supercooled liquid.[14] Thus this conductivity relaxation (c relaxation) provides another tool to help us understand the physics responsible for α relaxations. We have been able to use these data to extend our range of frequency and temperature for the primary-relaxation phenomena.

In this paper we present the frequency-dependent dielectric response of a liquid mixture of benzyl chloride and toluene. The data cover a wide temperature range, from the high-temperature liquid state to far below the glass transition temperature. This paper is organized as follows. In Sec. II we describe the experimental techniques used to measure the dielectric response over a very broad frequency range. We also describe the sample preparation. Section III contains the main experimental results along with a detailed discussion of the data analysis which includes the α, β, and c relaxations. In Sec. IV we compare the data for different chlorotoluene molecules in order to explain the origin of β relaxation. Finally we will report the results of a nonlinear dielectric-susceptibility measurement in Sec. V.

II. EXPERIMENTAL TECHNIQUE

A. Technique

We measured the complex dielectric constant $\epsilon=\epsilon'+i\epsilon''$ by placing the sample in a capacitor formed in the gap between two coaxial metal cylinders. The capacitance is about 20 pF in vacuum. The frequency-dependent dielectric susceptibility gives both the mean relaxation time and the shape of the relaxation. The sample is in the liquid state at room temperature. To fill the capacitor we simply immersed the coaxial cylinders in the liquid. The outer cylinder was wrapped with a Nichrome heating wire. Two different thermometers were used. A Au-Fe thermocouple was placed in the liquid and a calibrated platinum resistance thermometer, which has higher accuracy at high temperatures, was embedded in the temperature control. The temperature difference between two thermometers gave the temperature gradient across the sample and also provided a method to determine whether or not the liquid was in equilibrium. The entire assembly was mounted in a copper can, which was cooled in a ^{4}He Dewar. A computer both controlled the temperature and logged the data.

Depending on the frequency range, the data were taken by different methods. For measurements between 10 kHz and 10 MHz, we used a Hewlett-Packard 4275A multifrequency four-probe LCR meter, which measures the capacitance and dissipative factor, proportional to ϵ' and ϵ''/ϵ', respectively. Over the range 1 mHz to 10 kHz, we employed a digital lock-in technique[15] to measure the currents through the sample. A sinusoidal voltage was applied across the capacitor with a Hewlett-Packard 3326A frequency synthesizer. A Keithley 427 current amplifier was used at the output of the capacitor. The signal was measured by a Keithley 194A high-speed digitizer. The computer stored the voltage readings and performed the Fourier transformation to calculate the in-phase and out-of-phase signals proportional to ϵ'' and ϵ', respectively. The digital lock-in technique is described in detail elsewhere.[15] A schematic diagram for the experimental apparatus is shown in Fig. 1.

We took data by ramping the temperature at a con-

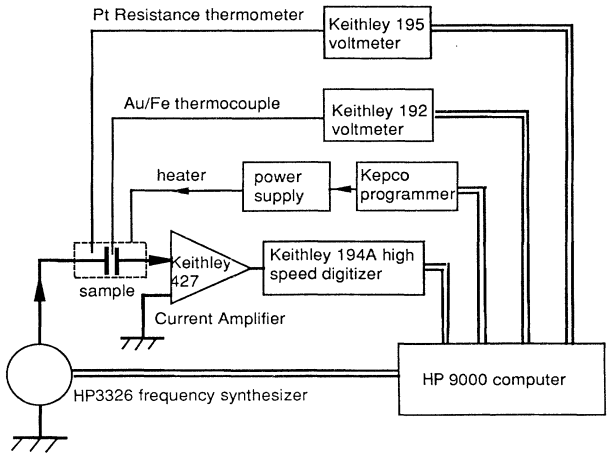

FIG. 1. A schematic diagram for the experiment. The double lines indicate IEEE-488 interface cables. The heavy lines indicate coaxial cables and the light lines indicate thermometers and/or heater wires.

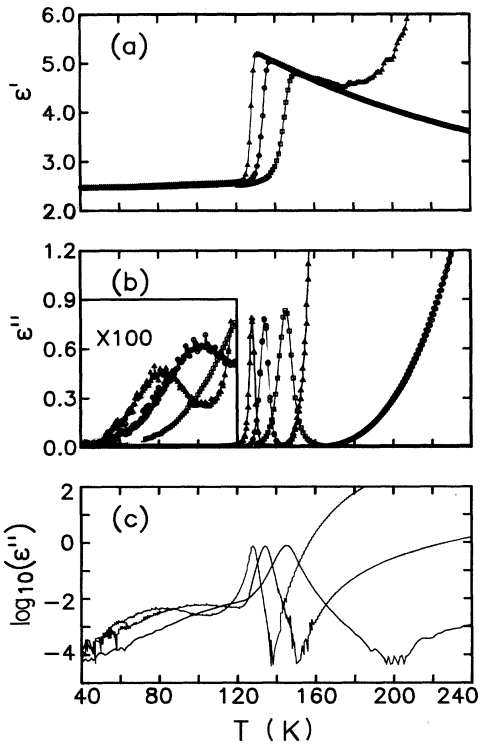

FIG. 2. Temperature-domain dielectric data for 25 vol% benzyl chloride in toluene. Graphs show (a) the real part ϵ', (b) the imaginary part ϵ'', and (c) $\log_{10}(\epsilon'')$ vs T for three frequencies. The inset of (b) has been multiplied by a factor of 100 so that we can see the β relaxations.

stant rate for a fixed frequency. The data above the glass transition temperature were taken as the sample was cooled down at a rate between 2 and 0.1 K/min. The rate depended on the measuring frequency and the temperature range. It is easier to avoid crystallization during cooling than during heating. The lower-temperature data were taken by warming up from liquid-He temperature. Upon warming, the sample always crystallized at 150 K, which is 25 K above T_g. Except within a few degrees Kelvin of T_g, the data are identical for the cooling and warming runs as long as no crystallization occurs. Close to T_g, the sample can be out of equilibrium. In that region, the warming runs were used. Representative plots of temperature-domain data are found in Fig. 2. We normalized the raw data to have $\epsilon''=0$ and to have the same value for ϵ' at liquid-He temperature since the gain and phase of the amplifier varies slightly with frequency. The frequency-dependent dielectric data can be taken by making constant-temperature cuts through the temperature-domain data.

B. Sample

The structures of molecular glasses are very complicated and difficult to deal with theoretically owing to our ignorance of their microscopic local structure. Nevertheless we still wish to find a simple molecular liquid in order to get a better idea of the underlying physics of the relaxation phenomena. Benzyl chloride (α-chlorotoluene) is a good candidate. The structure of this molecule is similar to toluene except that one hydrogen in the CH_3 group is replaced by a chlorine atom. We will show later that the experiments suggest that β relaxation is due to the rotation of this CH_2Cl group. The sample we used is a mixture of benzyl chloride and toluene. This mixture is used because it readily forms a glass even at very slow cooling rates. We found that the mixture of 25 vol% benzyl chloride with 75 vol% toluene (in volume) is the best glass-forming composition. The purities for toluene and benzyl chloride are greater than 99.7% and 98.5%, respectively.

III. DATA ANALYSIS AND DISCUSSION

A. General

We have measured the dielectric response of a mixture of 25 vol% benzyl chloride with 75 vol% toluene. The data cover the ten decades of frequency from 1 mHz to 10 MHz. The real, ϵ', and imaginary, ϵ'', dielectric response as a function of temperature are shown in Figs. 2(a) and 2(b), respectively, for three different frequencies, 100 mHz, 100 Hz, and 100 kHz. Since the magnitudes for the different relaxations vary enormously, we plot ϵ'' on a logarithmic scale in Fig. 2(c) so that all three relaxation phenomena are visible. For each type of relaxation, the lower-frequency loss peaks are always at lower temperatures. The primary relaxations approach T_g as the frequency is decreased. Just below the α relaxation there is a broader β relaxation. The β relaxation is about 100 times smaller than the α relaxation and is shown in the inset of Fig. 2(b). At high temperatures, the imaginary part of the dielectric response increases rapidly and is inversely proportional to the frequency. As we mentioned above, this is due to a small concentration of mobile impurity ions which are free to move in response to an electric field. The conductivity term will contribute to the imaginary part of dielectric response as σ/ω. In order to analyze this conductivity relaxation, we work with the complex electric modulus.[13] We define $M^*=1/\epsilon^*$ so that

$$M^*=\frac{\epsilon'}{(\epsilon')^2+(\epsilon'')^2}-\frac{i\epsilon''}{(\epsilon')^2+(\epsilon'')^2}=M'+iM'' .$$

The real and imaginary parts of the temperature-dependent modulus for one frequency (0.1 Hz) are shown in Fig. 3. Three different relaxation peaks—namely, conductivity relaxation (c relaxation), α relaxation, and β relaxation—can be discerned very clearly in the imaginary part.

The frequency-dependent data have been obtained by making constant temperature cuts through the temperature-domain data. One example for M'' versus $\log_{10}(\nu)$, is shown in Fig. 4. The c relaxation has a Debye form. The α relaxations are wider than the Debye form and can be fitted to a stretched-exponential function for low frequencies. In Fig. 4(b) the data are plotted on a logarithmic scale in order to make the β relaxation more

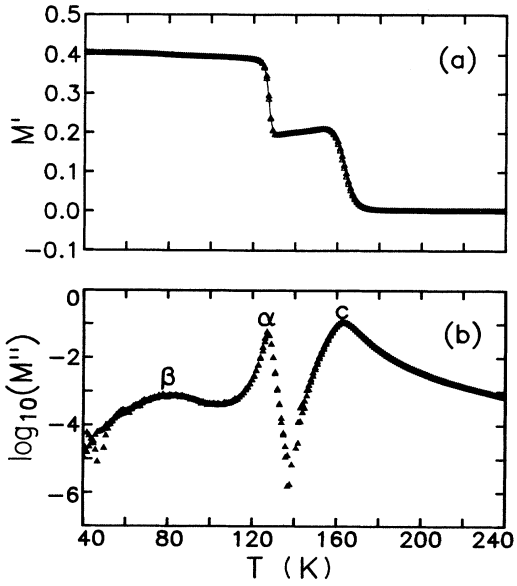

FIG. 3. The real part M' and the log of the imaginary part, $\log_{10}(M'')$, of the modulus vs temperature at 0.1 Hz. Three different loss peaks, corresponding to c, α, and β relaxations, are seen in (b).

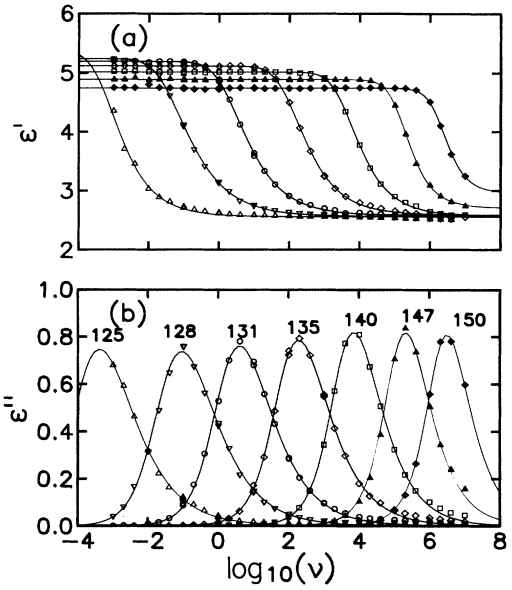

FIG. 5. The real ϵ' and imaginary ϵ'' parts of ϵ^* vs $\log_{10}[\nu(\mathrm{Hz})]$ at the labeled temperatures for the α relaxations. The curves are the best fits to the data using the stretched-exponential function.

apparent. The high-frequency β relaxations are much broader than the others. They appear to be symmetric functions so that they cannot be fitted by a stretched-exponential form. A detailed analysis of these different peaks is described below.

B. α relaxation

In Fig. 5 we present ϵ' and ϵ'' for 25 vol% benzyl chloride in toluene close to the glass transition temperature where the primary, or α, relaxation is important. The frequency range covers from 1 mHz to 1 MHz. Clearly the peaks in ϵ'' are broader than a Debye function which has a frequency width of $W_D = 1.14$ decades. The peaks in the data are also asymmetrical. The solid curves drawn through the data are fitting curves using the stretched-exponential function. The fitting is reasonably good around the peak position. The fits become poor in the high-frequency tails; in this region, there is also a contribution from the β relaxation.

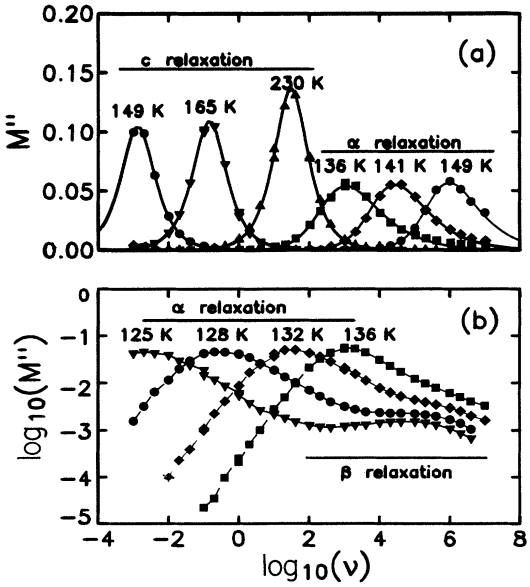

FIG. 4. Frequency domain data of M''. (a) has conductivity relaxation and α relaxation at the labeled temperatures. (b) is plotted on a logarithmic scale since the β relaxation is two orders of magnitude smaller than the α relaxation.

For the α relaxation we do not show any plots of the modulus versus $\log_{10}(\nu)$. Basically they are quite similar to the plots for ϵ^* and can also be fitted by a stretched-exponential form fairly well at the peak. (In such plots the peak position is shifted by $\tau_M = \tau_\epsilon \epsilon_0 / \epsilon_\infty$.)

Even though the stretched-exponential fit cannot describe the relaxation response over the whole frequency range, we can still obtain useful information from the fitting parameters. The peak frequency (ν_p) and normalized width $w = W/W_D$ (where W is the full width at half maximum in decades, and $W_D = 1.142$ is the Debye width) can be obtained from the fitting parameters $(1/\tau, \beta)$ very accurately over the range of β we used by[16]

$$\log_{10}(\nu_p) = \log_{10}(1/\tau) - 0.26(1-\beta) ,$$

$$1 - w^{-1} = 0.955(1-\beta) .$$

The plot of $\log_{10}(\nu_p)$ versus (1000 K)/T for the α relaxation is shown by the squares in Fig. 6. The solid curve is a fit to the data with the Vogel-Tamman-Fulcher form,

$$\nu_p = \nu_0 \exp\left[-\frac{E}{k(T - T_0)} \right] .$$

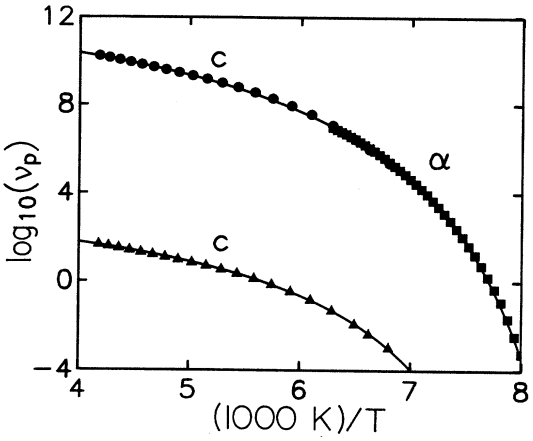

FIG. 6. Plot of $\log_{10}(\nu_p)$ vs (1000 K)/T for both c relaxation (triangles) and α relaxation (squares). The circles show the values of ν_p for the c relaxation multiplied by a constant as discussed in the text. The curves are the best fits to the Vogel-Tamman-Fulcher form and the parameters are listed in Table I.

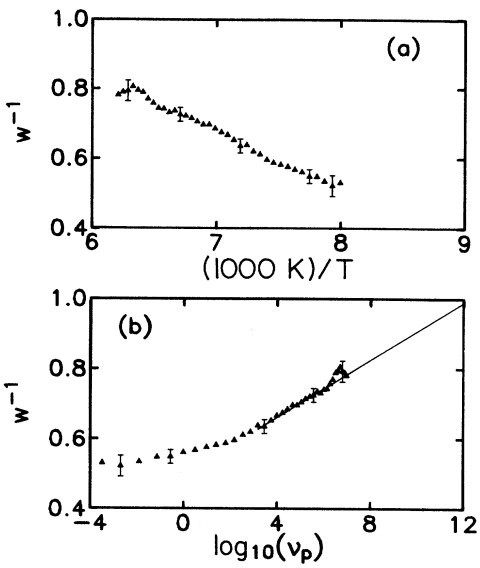

FIG. 7. The inverse of the normalized width, w^{-1}, vs (a) (1000 K)/T and vs (b) $\log_{10}(\nu_p)$.

The fitting parameters are listed in Table I.

We show the inverse of the normalized width, w, versus (1000 K)/T in Fig. 7(a) and versus $\log_{10}(\nu_p)$ in Fig. 7(b). The width of the peaks increases when the temperature is cooled toward the glass transition. If we extrapolate the data in Fig. 7(b) to a typical phonon frequency, 10^{12} Hz, we find that the normalized width approaches 1 (i.e., a Debye form).

Recently[4] it was shown that the dielectric susceptibility for molecular glasses can be scaled onto a single universal curve. This universal form of the α relaxation does not depend on the sample or the temperature. We plot our α relaxation data using the same scaling procedure and compare with the master curve in Fig. 8. The data can be scaled very well on this plot from far below zero in the scaled frequency units up to a high-frequency value of about 4. The deviations from the master curve (dashed line) at the high-frequency range depend on the temperature. These bumps are the β-relaxation peaks which appear in the same frequency range as the α-relaxation spectra.

C. c relaxation

The conductivity relaxation due to mobile ions in viscous liquids has been studied in ionic glasses.[17] The relaxation appears similar to the primary relaxation. Actually the conductivity relaxation can be observed in almost any liquid or glass, since the ionic impurities always contribute to the conductivity in the dielectric measurements at high temperature. The ionic motion can be described by the Stokes-Einstein equation $D=kT/6\pi\eta r$, in which η is the viscosity, D is the diffusion coefficient of the ions, and r is the ionic radius. The electrical conductivity due to the ionic diffusion can be derived from the Einstein-Nernst equation, which relates ionic conductivity to the diffusion by $\sigma/D=ne^2/kT$. This suggests that

TABLE I. Fitting parameters for three different relaxations. The c and α relaxations are fitted by the Vogel-Tamman-Fulcher form $\nu=\nu_0\exp[-E/k(T-T_0)]$. The β relaxation is fitted by an Arrhenius form $\nu=\nu_0\exp(-E/T)$.

Relaxation	$\log_{10}(\nu_0)$	E/k (K)	T_0 (K)
c relaxation	3.5	525	113
α relaxation	12.2	610	108
β relaxation	14.5	2805	

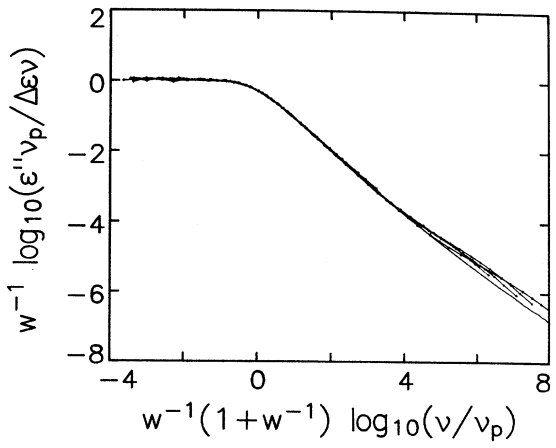

FIG. 8. The scaling plot of the frequency-dependent dielectric data (see Ref. 4). The solid line is a universal curve found for many glasses in Ref. 4 which have no β relaxation. The deviation from the master curve is due to the β relaxation.

there is a connection between the primary-relaxation time and the electrical-conductivity-relaxation time. Each relaxation time is defined by the ratio of the ordinary linear-response coefficient (viscosity or resistivity, respectively) to the appropriate modulus:

$$\tau_s=\eta/G_\infty, \quad \tau_\sigma=\rho/M_\infty ,$$

and

$$\frac{\tau_s}{\tau_\sigma}=\frac{ne^2}{6\pi r}\frac{M_\infty}{G_\infty} ,$$

where G_∞ is the infinite-frequency shear modulus, and M_∞ is the electrical modulus, $M_\infty=\epsilon_\infty^{-1}$.

In our measurement of the c relaxation, we find that M'' can be fitted to a Debye function as has been shown in Fig. 4(a). This implies that the ionic relaxation is decoupled from the α relaxation and that only the dc conductivity is important. For this case the dielectric response can be written as

$$\epsilon=\epsilon_\infty-i\sigma/\omega ,$$

and the imaginary part of modulus has the Debye form

$$M''=M_\infty\frac{\omega\tau_\sigma}{1+(\omega\tau_\sigma)^2} .$$

The significant feature of M'' is that it exhibits a peak centered at $\omega\tau_\sigma=1$. The apparent relaxation time here is $\tau_\sigma=\epsilon_\infty/\sigma$. M'' has a simple Debye form independent of whether or not there is a distribution of microscopic relaxation times.

In Fig. 9 we have shown the dielectric data for different temperatures as a function of frequency. The abscissa is scaled by the peak position of the α relaxation. The conductivity contribution on the low-frequency side of the figure can also be scaled on a straight line. This indicates that the conductivity relaxation is the same as the structural relaxation. The slope of the straight line is -1, suggesting that the conductivity is frequency independent and that the intercept at $\log_{10}(\nu/\nu_p)=0$ gives the ratio of the c to the α relaxation. We find $(6\pi r/ne^2)G_\infty/M_\infty\approx 3\times 10^8$. The peak frequencies for the c relaxation are shown in Fig. 6. If we multiply these values by this factor 3×10^8 (which amounts to a rigid vertical shift on this log-log graph), we get the circles which are a smooth continuation of the α-relaxation behavior. The Vogel-Tamman-Fulcher fit parameters are listed in Table I and compared with the α-relaxation parameters. The values of T_0 and E obtained from both sets of data are very close to each other, from which we infer that both sets of data measure the same relaxation phenomena.

D. β relaxation

Even though β relaxation has been observed for many years in many different glasses and polymers, there has been little analysis of the data in the frequency domain as we have done for the α relaxation. Because the β relaxation is very broad, one needs to cover a very wide frequency range, e.g., more than eight decades, to see the entire shape of the curve. Our digital lock-in technique enables us to cover more than ten decades. Another difficulty is that the β relaxation is much smaller than the α relaxation (in our sample it is 100 times smaller) and it overlaps with the α relaxation. One cannot separate them cleanly unless we know the exact functional form for the α relaxation at high frequencies. Here we will use the master curve obtained in other glasses for the shape of the α relaxation. In Fig. 10 we plot $\log_{10}(\epsilon'')$ versus $\log_{10}(\nu)$ for one temperature. We first measure the peak frequency and width of the main peak which is due to the α relaxation. This gives us the parameters $(\log_{10}(\nu_p), w)$. With these same parameters we get the pure α-relaxation curve from the master plot, which is shown as the solid

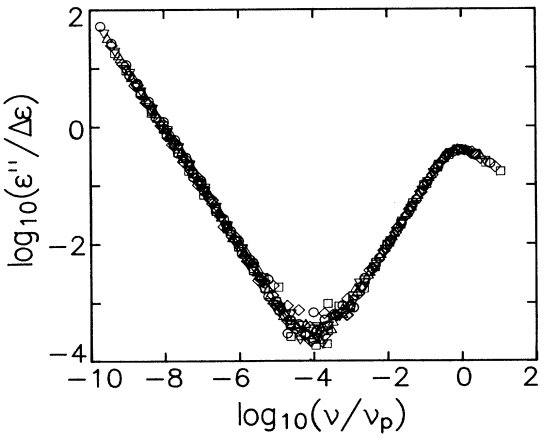

FIG. 9. The normalized imaginary part of the dielectric data $\epsilon''/\Delta\epsilon$ has been scaled by peak frequency of the α relaxation. Note that the ionic conductivity contributions are also scaled onto a single line.

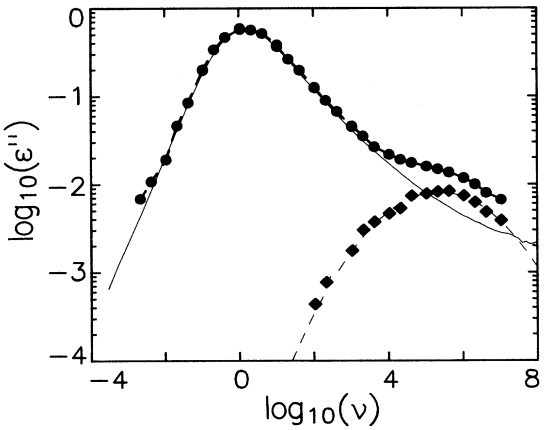

FIG. 10. The circles show the ϵ'' data for one temperature. The solid line shows the form obtained from the universal curve for the values of peak frequency and width given by the main peak of data. The diamonds show the result of subtracting the solid line from the ϵ'' and show contribution of the β relaxation. The dashed line is a log-normal fit to the β-relaxation data.

line. We subtract this α-relaxation curve from the data and obtain the pure β-relaxation peak. For the low-temperature data ($T<T_0$), the β relaxation does not overlap with the α relaxation (which does not exist in that temperature range). We found that both the low- and high-temperature β-relaxation peaks have a similar shape, i.e., very broad and symmetrical. A log-normal fit has been used to fit the β-relaxation peaks in a glassy crystal[10,11] and has the form

$$\epsilon(\omega)=\frac{\epsilon_0-\epsilon_\infty}{\sqrt{\pi}W}\exp\left[-\frac{[\log_{10}(\nu)-\log_{10}(\nu_p)]^2}{W^2}\right].$$

The β-relaxation peaks in our sample can be fitted by this same log-normal function and are shown as a dashed line in Fig. 10. We fit all of our β-relaxation data with this same form in Fig. 11. Clearly the width becomes broader as the temperature decreases. This log-normal form can be obtained[10,11] from a Gaussian distribution of energy barriers. We write

$$\epsilon(\omega,T)=\epsilon_\infty+(\epsilon_0-\epsilon_\infty)\int dE\frac{1}{\sqrt{\pi}\sigma}e^{-(E-E_0)^2/\sigma^2}\times\frac{1}{1-i\omega/\omega_0 e^{E/kT}}.$$

The width of energy-barrier distribution can be found from $\sigma=WkT\ln 10$ and the peak energy E_0 can be found from the slope of the Arrhenius plot.

The log-normal fit parameters are shown in Fig. 12. We also plot the peak frequency and width of α and c relaxations in the same figure for comparison. For the β relaxation the $\log_{10}(\nu_p)$ versus (1000 K)/T has an Arrhenius form $\nu_p=\nu_0\exp(-E/kT)$. The width linearly decreases with $1/T$ and is much larger than for the α relaxations and the Debye function ($w=1$). In Fig. 13 we plot σ versus T. We find that σ is almost constant with a small linear temperature dependence. The best fit is given by $\sigma=1214-4.55T/(1\text{ K})$. A similar decreasing width of the energy-barrier distribution was found[10,11] for the β relaxation in the glassy crystal $(KBr)_{1-x}(KCN)_x$. The static susceptibility strength $(\epsilon_0-\epsilon_\infty)$ does not depend on the temperature and has a value of 0.038 ± 0.001.

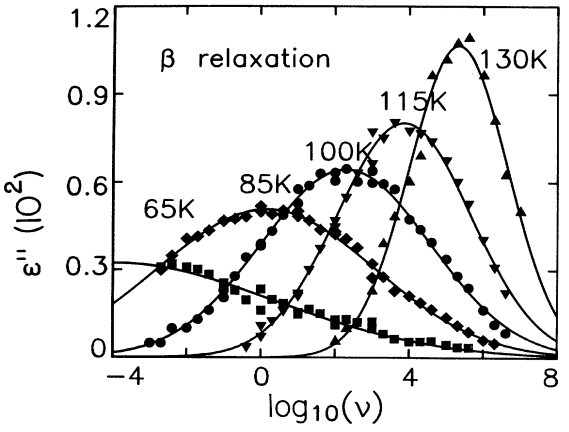

FIG. 11. ϵ'' vs $\log_{10}(\nu)$ for the β-relaxation data at different temperatures. Above 110 K, the data were obtained using the procedure shown in Fig. 10. All of the data could be fit to log-normal form (the solid lines).

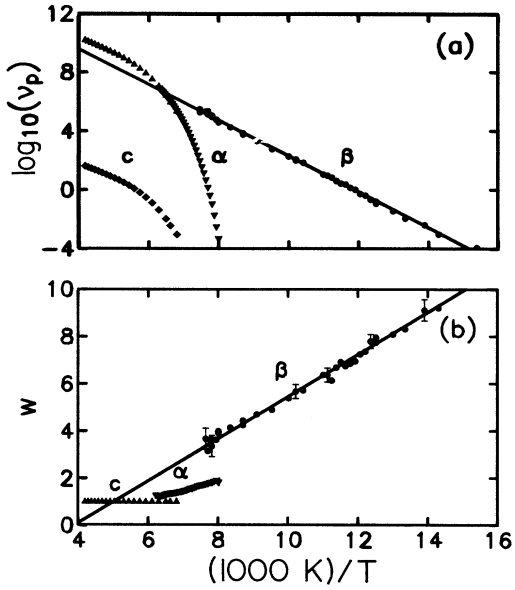

FIG. 12. The fitting parameters (a) $\log_{10}(\nu_p)$ and (b) the width w vs (1000 K)/T for three different relaxation processes. Notice that in (a) the α relaxations intersect the Arrhenius extrapolation of the β relaxation at high temperature (156 K).

We emphasize that the peak frequencies and widths are consistent with both the high-temperature data (where the β relaxation was separated from the α relaxation using the master curve) and the low-temperature data (where no deconvolution was necessary). This gives us confidence in our subtraction technique using the master curve.

Another important issue is how the α and β relaxations merge at high temperature and frequency. We find that the two curves for $\log_{10}(\nu_p)$ versus $1/T$ will cross at high frequency if we extrapolate the β-relaxation curve to a frequency slightly higher than was experimentally accessible. This crossing temperature is about 156 K as compared with $T_g=124$ K (at $\tau=10^4$ sec) and $T_0=108$ K.

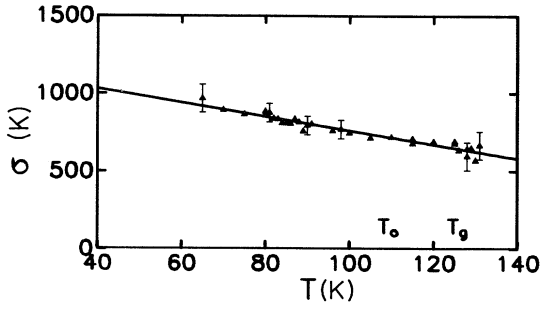

FIG. 13. Width of the energy-barrier distribution σ vs T.

This implies that the two relaxations have different origins. This result is in disagreement with the often-shown schematic diagram where the two relaxations merge.

IV. COMPARISON OF DIFFERENT CHLOROTOLUENE LIQUIDS: THE ORIGIN OF THE β RELAXATION

In order to understand what causes the β relaxation in this glass, we have studied a few different chlorotoluene molecules which have similar structures. The molecular structures are shown in Fig. 14. In each case the chlorine substitutes for a hydrogen atom at a different site in the toluene molecule.

We measured the dielectric response for the three different samples, α-, 2-, and 4-chlorotoluene. As shown in the figure, the dielectric response for the 4-chlorotoluene comes from the flip of the entire molecule. The response for the 2-chlorotoluene has a contribution from the rotation of the whole molecule along the long axes. α-chlorotoluene (benzyl chloride) has, besides this same contribution due to the rotation of the entire molecule about the log axis, an additional mode which comes from the rotation of the CH_2Cl subgroup.

In Fig. 15 we show ϵ'' versus T/T_m for different samples at one frequency (10 kHz). The temperature is normalized by the melting temperature. Significant secondary relaxation is found only for benzyl chloride and is due to the rotation of the CH_2Cl group. Since 2-chlorotoluene and 4-chlorotoluene do not have such a peak, we conclude that the rotation and flip of the whole molecule is very unlikely in those samples. This suggests that the β relaxation of the glass is mainly due to the rotation of the CH_2Cl subgroup. We also find that the energy-barrier distribution in the sample we have studied in the rest of this paper, 25 vol % benzyl chloride in toluene, is much broader than for pure benzyl chloride. Presumably this is due to the greater disorder in the mixture than in the pure liquid.

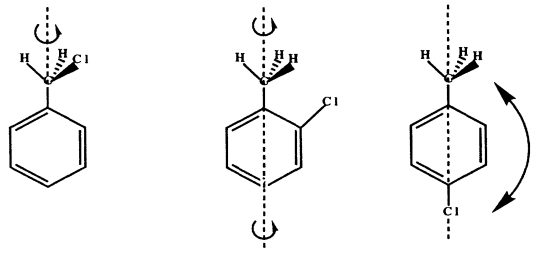

FIG. 14. The illustration of the molecular structures for a set of chlorotoluenes. The arrows indicate the various rotations that would contribute to the dielectric response in each molecule.

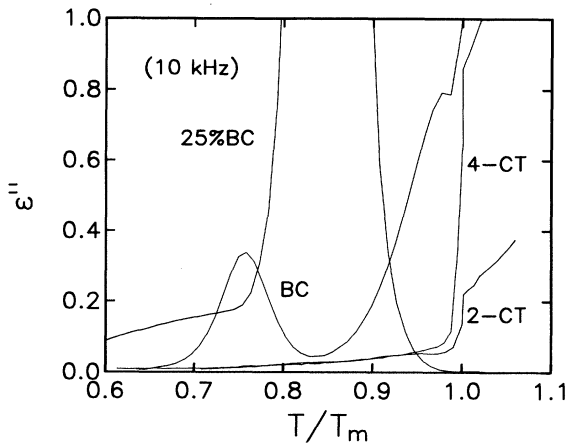

FIG. 15. The dielectric loss ϵ'' for several similar molecular liquids: 2-chlorotoluene, 4-chlorotoluene, α-chlorotoluene (benzyl chloride), and 25 vol % benzyl chloride in toluene. The abscissa is the temperature normalized by melting temperature, T/T_m. The graph shows that the β relaxations are due to the rotation of the CH_2Cl group rather than due to the flip or rotation of the whole molecule.

V. NONLINEAR DIELECTRIC SUSCEPTIBILITY

It is still not clear whether the transition from a supercooled liquid into glass is a true underlying phase transition as has been suggested by some theories[18–20] or whether it is just a dynamical freezing as explained by mode-coupling theory.[21] If there is a true underlying phase transition, some correlation length should diverge at the glass transition. In disordered systems it is sometimes necessary to measure the nonlinear susceptibility in order to couple to correlation length. For example, in spin-glass systems,[22] higher-order terms in the expansion of the equation of state in powers of the magnetic field

$$M/H=\chi_0-\chi_{\rm nl}H^2+O(H^4)$$

are related to the correlation length. Both the nonlinear susceptibility and the correlation length diverge at the transition temperature:

$$\chi_{\rm nl}=[(T-T_f)/T_f]^{-\gamma},$$

$$\xi=[(T-T_f)/T_f]^{-\nu}.$$

In order to look for a divergence of the correlation length, we have measured the nonlinear dielectric response in our sample, 25 vol % benzyl chloride in toluene. We define the nonlinear dielectric constant in the same way as in the magnetic susceptibility:

$$D/E=\epsilon^*-\epsilon_{\rm nl}E^2+O(E^4),$$

where ϵ^* is the linear dielectric response and $\epsilon_{\rm nl}$ is the first nonlinear term. When a large sinusoidal electric field at frequency ν is applied to the sample, one can get, in addition to a signal at ν, higher harmonic signals at 3ν, 5ν, etc. These higher-harmonic terms are much weaker

than the fundamental and for small electric fields only the fundamental can be measured. When the electric field is high enough, we can observe a 3ν signal which corresponds to the nonlinear susceptibility. In order to get good-quality data, one needs a very large electric field. A simple way to do this is to place two capacitor plates close to each other with a very small gap in between. The capacitor plates have to be very stable since any vibration or drift of the plates can overwhelm the signal. In our experiment we coat a window glass with a specially designed chromium pattern. The structure consists of two tiny needles very close together with a gap of 2 μm. Since one pair of needles does not produce sufficient signal, we place about one million such pairs on a single chip and immerse the chip in the sample liquid. We found the capacitance is very stable. We apply a 10 V sinusoidal voltage across the gap which produces a very large electric field of 5×10^6 V/m. We measure both the 1ν and 3ν harmonic current through the sample by digital lock-in techniques.

The result for a frequency of 1 Hz is shown in Fig. 16. The nonlinear term does not diverge as the temperature is decreased. This is consistent with an earlier experiment[23] which also found no divergence of the nonlinear susceptibility in a glass. Monroe has argued[24] that the correlation length will not be seen in the nonlinear susceptibility of the glass and electron glass systems. These results are consistent with his argument.

A divergent correlation length in a glass has not yet been observed. An experiment[25] which employed polystyrene spheres of various sizes in order to probe the viscosity of an organic glass former at different length scales also gave a negative result. Recently a computer simulation of the glass transition has been used[26] in order to look for a correlation length in both the density-density and bond-orientational correlation functions. The results show that neither type of order yields any evidence of a length-scale-dependent freezing as the simulated system is cooled towards T_g.

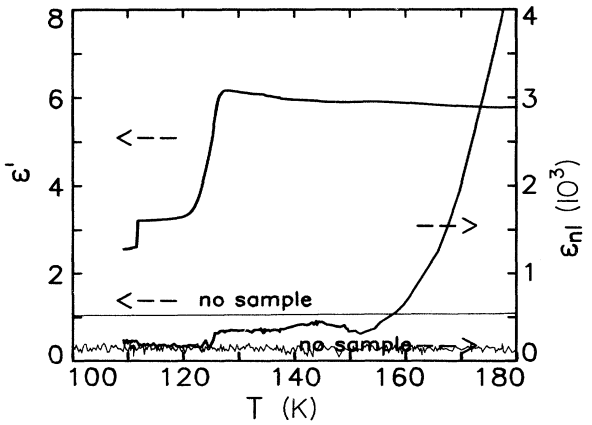

FIG. 16. The linear (ϵ') and nonlinear (ϵ_{nl}) susceptibility of 25 vol% benzyl chloride in toluene. The curves labeled "no sample" show the background signal due to the substrate holding the capacitor film.

VI. SUMMARY

We have measured three different relaxation phenomena in an organic molecular liquid. We found that the α-relaxation time diverges as the temperature decreases towards T_0 in a Vogel-Tamman-Fulcher fashion. The width of the relaxation peak is narrower at higher frequency and approaches a Debye form if extrapolated to a typical phonon frequency.

Mobile ionic impurities exist in the liquid above the glass transition. Their motion gives rise to conductivity relaxation at a frequency eight decades lower than is seen in the α relaxation. The two relaxations diverge at the same temperature. A scaling plot shows that the difference between the relaxation times determined by these two probes is a constant factor and indicates that both phenomena are governed by the same relaxation mechanism. We have used the data in the c relaxation in order to extend the high-frequency range of the α-relaxation data.

In the past year, a universal scaling behavior for the α relaxation in glass systems has been discovered. The master curve is different from any of the theoretical forms suggested in the literature (which always depart from the experimental data at high frequencies). This master curve of α relaxation enables us to identify and separate cleanly the β relaxation in the region where the α and β relaxations overlap. The β relaxation is due to the rotation of the subgroup CH_2Cl over a distribution of energy barriers. The results show that the response of the β relaxation has a log-normal form, which indicates that the distribution of these energy barriers is Gaussian. The relaxation time for the β relaxation exhibits an Arrhenius behavior in its temperature dependence. We can extrapolate this behavior to slightly higher temperatures and find that α and β relaxations cross. This is in disagreement with the often-shown schematic diagram where the two relaxations merge at high temperatures and frequencies. Similar behavior has been observed in ionic glasses where the fast and slow modes in the conductivity relaxation cross at some temperature.[17]

The high-field dielectric measurement shows that there is no divergent nonlinear dielectric response as the temperature is decreased to the glass transition temperature. Other experiments and computer simulations also fail to find evidence for a divergent correlation length. However, one may argue that because the phase transition temperature T_0 is far below the glass transition temperature T_g, the correlation length may still be short in the region that is experimentally accessible. There is no experimental evidence to preclude this possibility so that we must consider whether there is a true underlying phase transition to be an open question.

ACKNOWLEDGMENTS

I would like to thank P. K. Dixon, R. M. Ernst, L. P. Kadanoff, C.-H. Liu, W. Luo, N. Menon, and X.-Z. Wu

for stimulating discussions. I would especially like to thank my advisor, Professor Sidney Nagel, not only for stimulating my interest in this subject and providing me with a continual stream of ideas, but also for the constant encouragement and support which he has provided over the last several years. This work was supported in part by the National Science Foundation under Grant No. DMR-88-02284.

---

*Present address: MIT 13-2062, 77 Massachusetts Ave., Cambridge, MA 02139.

[1]W. Kauzmann, Chem. Rev. **43**, 219 (1948); C. A. Angell and W. Sichina, Ann. N. Y. Acad. Sci. **279**, 53 (1976); G. P. Johari, in *Relaxation in Complex Systems,* edited by K. L. Ngai and G. B. Wright (McGregor and Werner, Washington, D. C., 1984).

[2]N. O. Birge and S. R. Nagel, Phys. Rev. Lett. **54**, 2674 (1985); N. O. Birge, Phys. Rev. B **34**, 1631 (1986); P. K. Dixon and S. R. Nagel, Phys. Rev. Lett. **61**, 341 (1988).

[3]D. W. Davidson and R. H. Cole, J. Chem. Phys. **19**, 1484 (1951).

[4]P. K. Dixon, L. Wu, S. R. Nagel, B. D. Williams, and J. P. Carini, Phys. Rev. Lett. **65**, 1108 (1990); L. Wu, P. K. Dixon, N. Menon, K. O'Brien, S. R. Nagel, B. D. Williams, and J. P. Carini (unpublished).

[5]T. A. Litovitz, in *Physics of Non-crystalline Solids,* edited by J. A. Prins (North-Holland, Amsterdam, 1965), p. 220.

[6]Y. H. Jeong, S. R. Nagel, and S. Bhattacharya, Phys. Rev. A **34**, 602 (1986).

[7]P. B. Macedo and A. Napolitano, J. Chem. Phys. **49**, 1887 (1968); W. T. Laughlin and D. R. Uhlmann, J. Phys. Chem. **76**, 2317 (1972).

[8]D. J. Plazek and J. H. Magill, J. Chem. Phys. **45**, 3038 (1966); **46**, 3757 (1967).

[9]G. P. Johari and M. Goldstein, J. Chem. Phys. **53**, 2372 (1970); G. P. Johari, Ann. N. Y. Acad. Sci. **279**, 117 (1976).

[10]N. O. Birge, Y. H. Jeong, S. R. Nagel, S. Bhattacharya, and S. Susman, Phys. Rev. B **30**, 2306 (1984).

[11]L. Wu, R. M. Ernst, Y. H. Jeong, S. R. Nagel, and S. Susman, Phys. Rev. B **37**, 10444 (1988); R. M. Ernst, L. Wu, S. R. Nagel, and S. Susman, *ibid.* **38**, 6246 (1988).

[12]M. Goldstein, J. Chem. Phys. **51**, 3728 (1969).

[13]J. Wong and C. A. Angell, *Glass: Structure by Spectroscopy* (Dekker, New York, 1976), Chap. 11.

[14]G. Williams and P. J. Hains, Chem. Phys. Lett. **10**, 585 (1971).

[15]N. O. Birge and S. R. Nagel, Rev. Sci. Instrum. **58**, 1464 (1987); P. K. Dixon and L. Wu, *ibid.* **60**, 3329 (1989).

[16]P. K. Dixon, Phys. Rev. B **42**, 8179 (1990).

[17]C. A. Angell, Chem. Rev. **90**, 523 (1990).

[18]M. H. Cohen and G. S. Grest, Phys. Rev. B **20**, 1077 (1979).

[19]J. H. Gibbs and E. A. DiMarzio, J. Chem. Phys. **28**, 373 (1958); G. Adam and J. H. Gibbs, *ibid.* **43**, 139 (1965).

[20]D. L. Stein and R. G. Palmer, Phys. Rev. B **38**, 12035 (1988).

[21]S. P. Das and G. F. Mazenko, Phys. Rev. A **34**, 2265 (1986); **36**, 211 (1987); U. Bengtzelius, W. Gotze, and A. Sjolander, J. Phys. C **17**, 5915 (1984); E. Leutheusser, Phys. Rev. A **29**, 2765 (1984); G. H. Fredrickson and H. C. Andersen, Phys. Rev. Lett. **53**, 1244 (1984); T. R. Kirkpatrick, Phys. Rev. A **31**, 939 (1985).

[22]K. Binder and A. P. Young, Rev. Mod. Phys. **58**, 801 (1986).

[23]Y. H. Jeong and S. R. Nagel (private communication).

[24]D. Monroe (unpublished).

[25]P. K. Dixon, S. R. Nagel, and D. Weitz (unpublished).

[26]R. M. Ernst, S. R. Nagel, and G. S. Grest, Phys. Rev. B (to be published).